

Design and Development of the 3.2 Gigapixel Camera for the Large Synoptic Survey Telescope

S.M. Kahn^{*a}, N. Kurita^a, K. Gilmore^a, M. Nordby^a, P. O'Connor^b, R. Schindler^a, J. Oliver^c, R. Van Berg^d, S. Olivier^e, V. Riot^e, P. Antilogous^f, T. Schalk^g, M. Huffer^a, G. Bowden^a, J. Singal^a, M. Foss^a

and the LSST Camera Team

^aSLAC National Accelerator Laboratory, 2575 Sand Hill Road, Menlo Park, CA 94025

^bBrookhaven National Laboratory, PO Box 5000, Upton, NY 11973

^cHarvard University, Department of Physics, 18 Hammond St., Cambridge, MA 02138

^dUniversity of Pennsylvania, Department of Physics and Astronomy, 209 South 33rd Street Philadelphia, PA 19104-639

^eLawrence Livermore National Laboratory, 7000 East Avenue, Livermore, CA 94550

^fLaboratoire de physique nucléaire et de physique des hautes énergies, IN2P3 and UPMC, 4 Place Jussieu, Tour 12, 1er étage, 75252 Paris, Cedex 05, France

^gUniversity of California at Santa Cruz, Santa Cruz Institute for Particle Physics, 1156 High St., Santa Cruz, CA 95064

ABSTRACT

The Large Synoptic Survey Telescope (LSST) is a large aperture, wide-field facility designed to provide deep images of half the sky every few nights. There is only a single instrument on the telescope, a 9.6 square degree visible-band camera, which is mounted close to the secondary mirror, and points down toward the tertiary. The requirements of the LSST camera present substantial technical design challenges. To cover the entire 0.35 to 1 μm visible band, the camera incorporates an array of 189 over-depleted bulk silicon CCDs with 10 μm pixels. The CCDs are assembled into 3 \times 3 "rafts", which are then mounted to a silicon carbide grid to achieve a total focal plane flatness of 15 μm p-v. The CCDs have 16 amplifiers per chip, enabling the entire 3.2 Gigapixel image to be read out in 2 seconds. Unlike previous astronomical cameras, a vast majority of the focal plane electronics are housed in the cryostat, which uses a mixed refrigerant Joule-Thompson system to maintain a -100°C sensor temperature. The shutter mechanism uses a 3 blade stack design and a hall-effect sensor to achieve high resolution and uniformity. There are 5 filters stored in a carousel around the cryostat and the auto changer requires a dual guide system to control its position due to severe space constraints. This paper presents an overview of the current state of the camera design and development plan.

Keywords: LSST, camera, survey, wide-field, gigapixel, CCD

1. INTRODUCTION

The Large Synoptic Survey Telescope (LSST) has been designed to enable a wide variety of diverse scientific investigations, with particular emphasis on four general areas of research [1]:

- *Probing the nature of dark energy and dark matter* – The dynamical evolution of the universe is determined by the balance between the gravitational effects of dark energy and dark matter, neither of which is presently well understood. Very sensitive constraints on the properties of these two mysterious components can be derived from statistical analyses of the distributions of galaxy shapes, brightnesses, and positions out to high redshift. In addition, the acquisition of a large sample of Type 1a supernovae, which are calibratable standard candles, can be used to accurately calibrate the redshift-distance relation, which then allows us to infer the expansion history of the universe as a function of cosmic time.

- *Taking an inventory of the solar system* – The orbits of small-body populations, such as asteroids, trans-Neptunian objects, and comets, provide a fossil record of how the solar system was formed and evolved through accretion, collisions, and gravitational deflection by existing and vanished giant planets. Such orbits can be detected and mapped through a series of multiple exposures of a major fraction of the sky separated by timescales of minutes to years.
- *Exploring the transient optical sky* – A systematic search for variability down to faint limiting magnitudes can yield vital information for a large number of astrophysical topics, ranging from stellar evolution to the nature of active galactic nuclei. There are major gaps in our understanding of variability at optical wavelengths, since most of the sky has never been surveyed on the relevant timescales. A series of repeat exposures at different time intervals can go a long way to addressing this need. Very rare “events” can only be detected if this variability survey is conducted over a large fraction of the sky.
- *Mapping the Milky Way* – A detailed study of the structure and content of the Milky Way and its environment can provide key information on galaxy formation and evolution, as well as on the particular history of the galaxy in which we live. The major challenges in discerning the structure of the galaxy have always involved uncertainties in the distances for the vast numbers of stars that are detected. Through repeat exposures over a large fraction of the sky, we can infer distances through both parallax and proper motion measurements.

Somewhat surprisingly, the needs of all four of the investigations outlined above can be simultaneously met by a single synoptic survey performed over a large fraction of the sky ($\sim 20,000$ square degrees). However, the implications for the system design are daunting. It must have very large étendue ($\sim 300 \text{ m}^2 \text{ deg}^2$), and it must have the capability to make relatively short exposures (~ 15 s) with high efficiency. The LSST design has evolved to meet those requirements.

The detailed implications for the telescope and data management subsystems are described elsewhere in these proceedings [2, 3, 4]. Here we concentrate on the design constraints on the camera, which involve a number of technical challenges:

- *Large field of view* – To achieve the required étendue, the camera must have a very large field of view, 9.6 square degrees. With the fast f/1.2 optical design that has been adopted for LSST, this requires a physically large focal plane (64 cm diameter), with small pixels (10 μm), and tight tolerances on focal plane flatness ($\sim 15 \mu\text{m}$ peak-to-valley). This can only be achieved by mosaicking a large number of four-side buttable sensors, with narrow interchip gaps.
- *Wide spectral coverage* – The broad bandpass sampled by LSST (350 -1050 nm) necessitates the use of deep, fully depleted CCDs with minimal charge spreading, as well as the implementation of six distinct optical blocking filters with rapid interchangeability.
- *Fast readout* – To maintain high efficiency given the short exposures, the readout of the entire 3.2 Gpixel CCD array must be accomplished within 2 s. That requires a highly parallelized design with multiple readout ports per sensor. The large number of signal lines then motivates a modularized approach, where both the front end and back end electronics are tightly integrated with the sensor modules inside the cryostat.
- *Location of the camera within the telescope beam* – The full camera is located in the telescope beam just forward of the secondary mirror. To avoid vignetting, the outer envelope is thus tightly constrained. Heat dissipation to ambient must also be tightly controlled. Finally, since the power generation within the cryostat is substantial, a novel refrigeration design had to be adopted to handle the high heat loads without requiring the transport of a cold gas or liquid refrigerant all the way from the floor of the dome. The sheer size of the LSST camera introduces many additional challenges. The large refractive lens assembly, which forms the entrance window to the camera, is taller than the average woman. With 5'5" diameter and 12' length, the camera weighs 6610 lbs (Figure 1).

Below, we describe the key elements of the camera design and our current state of development for each of the major subsystems. We begin with a high level overview, and then continue with more detailed discussions of each of the individual components. Companion papers in these proceedings provide more in-depth discussions of selected aspects of the camera design and development program [5, 6, 7, 8, 9].

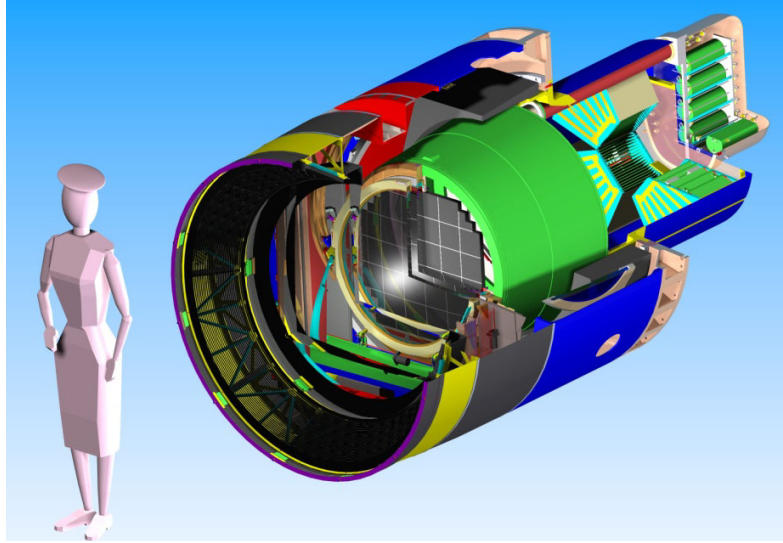


Figure 1. Cross-section of the camera.

2. OVERVIEW OF MAJOR CAMERA SUB-SYSTEMS

The main component of the camera is a cryostat, containing a focal plane array of 189 4K x 4K CCDs used for scientific imaging, 8 hybrid CMOS sensors for guiding and 4 split CCDs used for wavefront sensing (Figure 2). The CCDs are modularized for manufacturability and ease of maintenance into 21 science raft towers, which contain 9 sensors and their related electronics. The entrance beam is focused via three large refractive lenses, L1, L2, and L3, respectively. L1 and L2 are integrated as a single assembly, while L3 doubles as the entrance window to the cryostat. The shutter and optical blocking filter occupy a limited space between the L2 and L3 lenses. Five filters are stored on-board the camera in a storage carousel, with an auto changer that allows for quick filter changes during observing runs. An external filter exchanger allows a 6th filter to be exchanged for any one of the five during daylight hours. The shutter lies just behind the filter, providing accurate exposure control and blocking stray light from illuminating the focal plane when closed.

The entire camera assembly is fully enclosed and hermetically sealed to ensure light tightness and a clean and thermally stable environment. Ports and access holes are provided to service and maintain the hardware to minimize downtime. The camera is positioned in the middle of the telescope where the cross-sectional area is constrained by optical vignetting and where heat dissipation must be controlled to limit thermal gradients in the optical beam. The filter auto exchange system, shutter, and system electronics are accessible without having to dismount the camera from the telescope. A separate housing contains 8 refrigeration system heat exchangers which is part of the novel approach for dissipating the high thermal load in the cryostat.

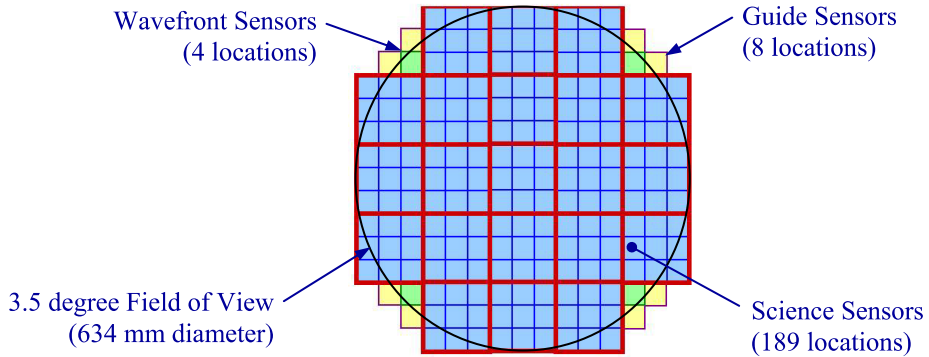


Figure 2. Focal plane geometry. Each blue square is a 4K x 4K CCD. The red squares indicate the raft boundaries.

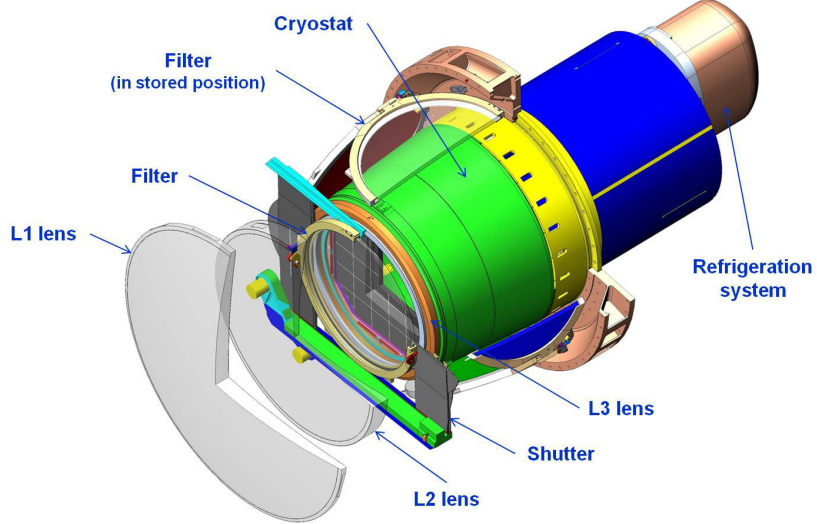


Figure 3. Camera schematic view.

3. SCIENCE SENSORS

The sensors are the single largest cost item in the camera budget, they are the highest-ranked technical and schedule risk, and they define the critical path for the LSST project as a whole [10].

The reference design for LSST sensors has been described previously [11, 12]. Briefly, it specifies an over-depleted silicon thickness of 100 μm (tradeoff of NIR QE and charge diffusion), flatness of 5 μm (to stay within LSST's small focal depth), a pixel size of 10 μm (0.2" at LSST's plate scale), and segmented full-frame architecture with sixteen amplifiers per CCD (to give 2 second readout with approximately 5 e- rms read noise). Figure 4 shows a layout of the readout geometry. High resistivity bulk silicon technology, seldom used in commercial CCDs, is required for this application. The package design is also critical for achieving the flatness, thermal stability, and close-butting requirements.

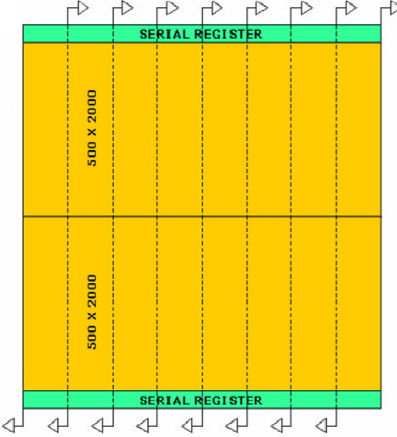


Figure 4. Readout geometry of the CCDs, indicating the 16 readout ports per sensor.

The LSST project has engaged two suppliers to investigate technical approaches to achieving the sensor requirements. Several pre-prototype demonstrator devices have been fabricated and tested, and initial characterization results have been reported previously [12]. Results to date on bulk high-resistivity silicon, room temperature chip flatness, and readout segmentation have been encouraging. Over the next 12 months the development effort will focus on demonstrating precision packages with flatness and alignment stability over the operational temperatures, speed/read noise performance, optimized antireflection coatings, and process reproducibility and robustness.

Two telescope test campaigns have also been carried out using single pre-prototype sensors and conventional readout electronics. A variety of astronomical targets were observed. Figure 5 shows an RGB image of the nearby galaxy NGC 891 obtained with these devices.



Figure 5. NGC 891, VRI composite image, obtained with a prototype LSST sensor.

4. RAFT TOWERS

The functions of the science raft tower are to provide:

- precise mechanical location and support for the CCD array;
- front end electronic support functions to control and read out the CCDs;
- thermal management of the CCDs and front end electronics.

Mechanical requirements are extremely stringent and include locating the CCD imaging surfaces to within a $6.5 \mu\text{m}$ flatness envelope with gaps of 0.25 mm between adjacent CCDs. As a result of the fine segmentation of the CCDs, the science raft tower has to implement all electronic functions of a 144-channel CCD controller in a volume contained within the footprint of the raft. Although low-power ASICs are used, their total power dissipation is significant and must be removed from the cryostat through adequate thermal paths. Finally, the imaging surfaces of the CCDs must be protected from contamination by condensable materials in the electronics enclosures.

Figure 6 illustrates the components of the science raft tower (SRT). The SRT is the modular building block of the camera focal plane and consists of three major assemblies:

- The raft-sensor assembly (RSA) is a 3×3 mosaic of science CCDs in precision packages mounted on a silicon carbide baseplate. The RSA also includes temperature sensors, make-up heaters, and flexible electrical and thermal connections.
- The front end cage (FEC) houses circuit boards with custom video processing and clock/bias buffering electronics and contains copper planes providing the thermal path for cooling the CCDs and electronics.
- The raft control crate (RCC) contains electronics for video digitizing, clock sequencing, bias generation, temperature sensing, and interfacing to the control and data acquisition systems.

The SRT is an autonomous, fully testable and serviceable camera capable of acquiring 144-Mpixel images in 2 seconds. It occupies a volume of about $13 \times 13 \times 28 \text{ cm}^3$ and dissipates over 25 W of power during readout.

All components of the SRT are contained within the camera cryostat vacuum space. The RSA and FEC are maintained at an operating temperature of around -100°C . This temperature is chosen as a compromise between sensor dark current

and near IR quantum efficiency. The RCC operates at a warmer temperature, around -40°C , to reduce the load on the cooling system and to allow the use of standard commercial electronics. To prevent volatile contaminants from condensing on the CCD imaging surfaces several precautions are taken: The PCBs in the FEC are conformally coated; the CCDs are never allowed to be the coldest surfaces in the cryostat; and the FEC includes a conductance barrier to minimize molecular flow towards the CCDs.

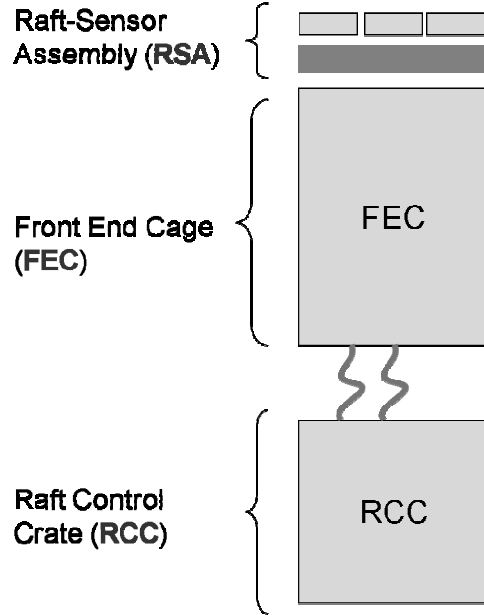


Figure 6: Components of the Science Raft Tower

All front end electronic functions are implemented as compact, ASIC-based circuit boards housed in the FEC and RCC. Figure 7 shows a block diagram of the electronics organization for three of the nine CCDs on a raft. Each CCD is connected to a pair of Front End Boards (FEB) by two flex cables with video, clock, and bias signals for eight amplifier segments. FEBs perform video signal processing and clock and bias analog buffering. Parallel and serial clocks are handled on alternate FEB's, and the parallel clocks are bussed across the CCD multilayer ceramic. Boards in the RCC contain analog-to-digital converters, FPGA-based clock sequencers, buffer memory, and a high-speed serial interface to the science data acquisition system. The RCC is also responsible for generating CCD bias voltages, reading temperature sensors, and providing current to makeup heaters in the tower.

Conceptual mechanical layout of the raft tower is shown in Figure 8. The nine CCDs are each fastened to a flat silicon carbide baseplate using three precision studs to achieve a coplanar surface and two close-fitting alignment pins to locate the CCDs laterally. The CCDs are cooled by conduction through a combination of their mounting studs and individual thermal straps to the raft baseplate. The raft baseplate in turn is cooled via flexible thermal straps which connect to thick copper planes in the FEC; these are bolted to a copper cryo plate with flowing cryogen. Electronics front end boards have heavy copper internal ground planes which are clamped at the board edges and bolted to the FEC thermal planes. Thermal sensors on each CCD and in several locations on the raft baseplate and front end boards provide temperature monitoring, and makeup heater resistors mounted on the raft baseplate control the temperature with a stability requirement of $\pm 0.1^{\circ}\text{C}$ over a 12-hour period.

Each CCD has two short flex cables which mate to nano-connectors on the front end boards providing the electrical interface. A conductance barrier (not shown) helps prevent any volatile contaminants from condensing on the CCD imaging surfaces.

The underside of the raft baseplate has three precision V-grooves which provide a kinematic coupling to spheres mounted on the cryostat grid. Spring-loaded arms pretension the kinematic couplings when the raft towers are integrated into the grid. A temporary rigid coupling of the RSA to the FEC is provided during tower assembly and transport. Other than this temporary coupling, all connections between the RSA and FEC are "soft" to allow relative motion during cooldown and to avoid applying bending moments to the rafts.

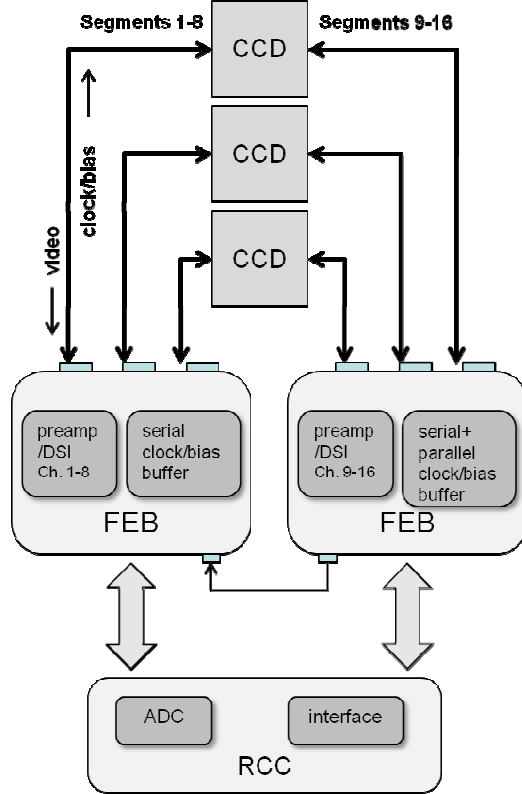


Figure 7. Science raft tower block diagram showing signal paths to/from three of the nine CCDs on a raft.

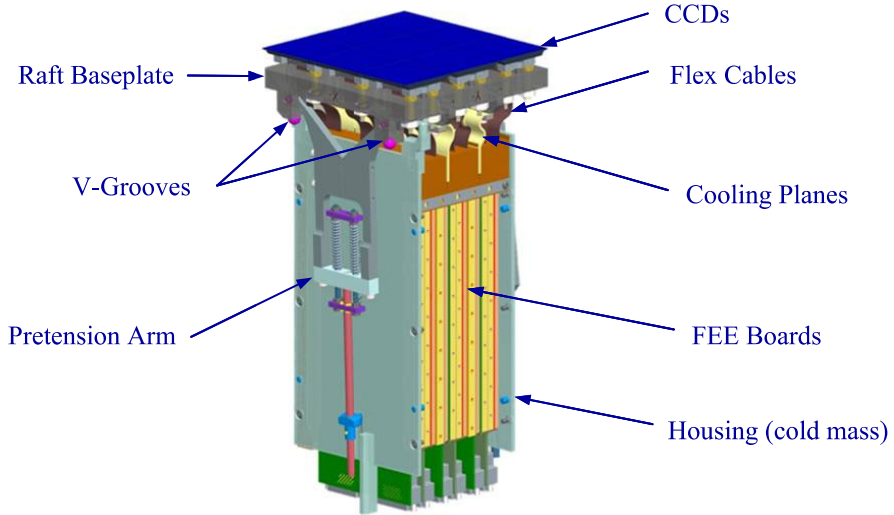


Figure 8. Conceptual mechanical layout of the Raft-Sensor Assembly (top) and Front End Cage.

Corner raft towers are located inside the cryostat at the four corners of the focal plane (Figure 2). The triangular rafts contain one wavefront sensor and two guide sensors, while front end electronics for them are packaged within the footprint of the triangular raft behind the focal plane. The guide sensors are outside the nominal field of view and the wavefront sensors are in an area that is substantially impacted by optical vignetting. The FEC and RCC for the corner raft operate at the same temperatures as the science rafts.

The corner raft curvature wavefront sensors acquire pixel data for the observatory active optics system. To support this activity, the corner rafts acquire intra- and extra-focal images from sensors 1 mm above and below the focal plane at 4 locations around the periphery of the focal plane. The split-offset device utilizes the current technology being developed for the science sensors. These images are used by the Telescope Control System to estimate the wavefront and, through reconstruction, provide inputs to the active optics controller. Images are collected in parallel with the science images and follow the corresponding exposure time and cadence.

The corner raft guide sensors acquire small images centered on selected bright stars at a nominal 9 Hz rate. The camera delivers centroids to the telescope to assist in guiding. This information enables the telescope guiding feedback loop to make small adjustments in response to wind buffeting, vibration, or slight inaccuracies of the telescope tracking. The guide sensors employ hybrid CMOS technology for fast windowed readout.

5. CRYOSTAT

The cryostat lies in the center of the camera. Its vacuum housing supports the focal plane that operates at -100°C, as well as the analog and digitizing electronics. The cryostat assembly serves three functions: providing structural support and isolation for the detector plane, maintaining thermal control of the detectors while removing the dissipated and radiative heat load, and ensuring that the detectors are in a clean operating environment.

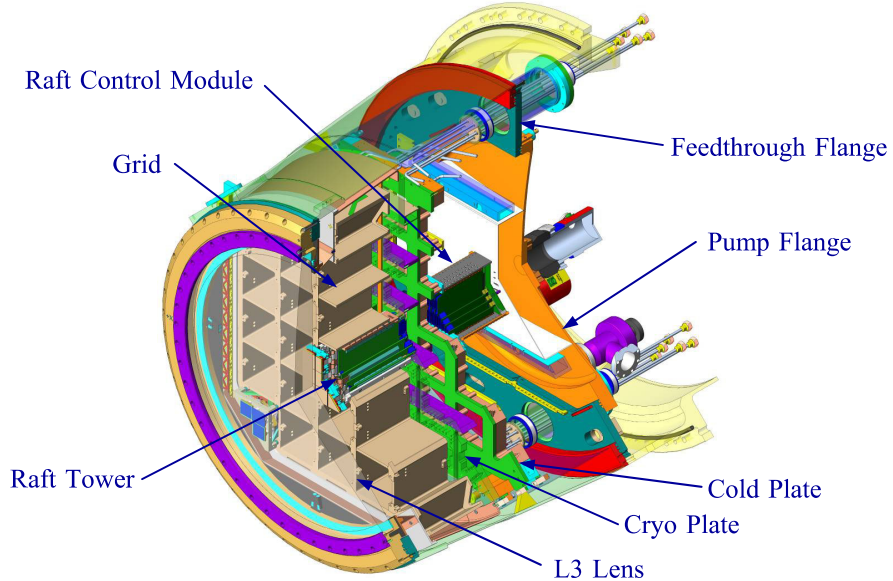


Figure 9. Assembled Cryostat with Raft Tower Inserted.

The cryostat is comprised of a conical vacuum housing, capped on the front end by the L3 lens assembly, and on the back end by feedthrough and utility bulkheads. Flexures mounted to the housing support the Cesic® grid assembly which stably supports and thermally isolates the CCD detectors on their rafts (RSAs). Behind the detector plane, the actively cooled cryo plate, removes process heat loads and provides structural support for the front end electronic cages (FECs), while providing a stable thermal environment for the grid and detectors. Further back in the cryostat, the cold plate similarly supports and cools the digitizing and control electronics (RCCs). At the back end of the cryostat, science and instrumentation signals pass through feedthroughs in the vacuum flange, along with cryogenic lines. Vacuum pumps and instrumentation are also located here, to help maintain the clean, cold environment.

The grid assembly provides stable support for the RSAs. This will be the first ground-based astronomy camera that employs a short carbon-fiber reinforced ceramic structure. Cesic® is chosen for the grid because of high stiffness-to-weight ratio, high thermal conductivity, low coefficient of expansion and manufacturability. Ball nests mounted to the grid form a kinematic interface to each of the detector rafts and copper cold straps ground the grid thermally to the cryo plate. The grid is supported off of the cryostat front flange by three titanium flexures that provide kinematic support and thermal and electrical isolation.

The cryo plate supports and cools the FECs, while also providing a stable thermal environment for the grid. At approximately -120°C , it will also be the coldest surface in the cryostat, helping reduce the detector cryo-pumping probability. The large copper plate includes stainless steel stiffening ribs to carry the weight of the electronics, and cooling channels for flowing refrigerant to remove the heat dissipated by the electronics. A cryo shroud mounts to the perimeter of the plate and extends forward around the outer and front faces of the grid, isolating it from radiative heating from the warm walls of the cryostat housing. The cryo plate and shroud assembly are mounted to the cryostat housing by four titanium flexures, while refrigerant supply and return lines enter and exit the cryo plate from vacuum-insulated feedthroughs at the rear of the cryostat.

The large copper cold plate supports and cools the digitizing, communication, and control electronics housed by the RCC using cryogenic refrigerant. The cold plate is also supported off the cryostat wall by four titanium flexures.

5.1 Refrigeration

Unprecedented heat loads in the cryostat have led to the development of a novel approach for the refrigeration system. The system must remove heat from four sources. The radiant heat load from L3 onto the detectors is 75 watts [13]. An additional 600 watt heat load comes from the front end electronics located directly behind the focal plane. Finally, an estimated additional 25 watts of heat leaks into the cryostat along internal structural supports. Furthermore, raft electronics (RCC) dissipate 400 watts at -40°C . LSST's total 1.1 KW cryostat heat load is an order of magnitude larger than previous cryogenic CCD cameras. A mixed refrigerant technology is under development and initial thermodynamic analysis shows that this is a promising solution.

For a 700 watt cryogenic load, traditional liquid nitrogen evaporative cooling would require 74 gallons/day; however, storage of this much cryogenic liquid on board the moving camera is not practical. On the other hand, delivering cryogenic refrigeration to the camera across the altitude and azimuth rotations of the telescope mount is a major problem for the refrigeration system. As a survey telescope, LSST will turn the equivalent of 10,000 revolutions on its azimuth mount over 10 years. Vacuum insulated flexible metal hose to carry cryogens across the two telescope mount rotations plus the camera's rotator is an equally high-risk. Thus, the decision has been made to confine the low temperature portions of the cooling system to the camera cryostat. Refrigeration based on vapor-compression and Joule-Thomson expansion will deliver room-temperature compressed liquid-vapor refrigerant to the camera through flexible synthetic hoses which easily cross the three camera and telescope mount rotations.

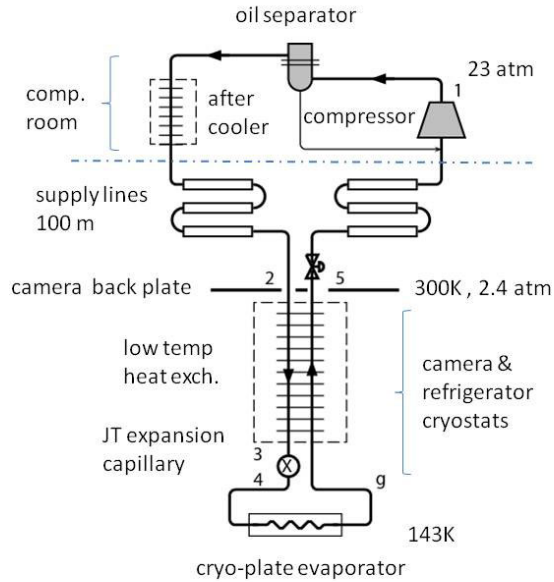


Figure 10. Camera refrigeration circuit.

The refrigeration system under development by *MMR Technologies* [14] is based on a refrigeration cycle similar to domestic kitchen refrigerators. It reaches cryogenic temperatures by using a proprietary mixture of common non-flammable fluoro-hydrocarbon refrigerants plus argon and nitrogen. A commercial 23atmosphere hermetic reciprocating

compressor with water-cooled aftercooler and oil separators is located in the observatory basement. Room-temperature supply and return lines, about 100 meters long, couple the compressor to a low temperature counter-flow heat-exchanger and expansion capillary mounted in a vacuum vessel behind the camera cryostat. Expansion and evaporation of pre-cooled high pressure refrigerant cools evaporator channels in the camera's cryo plate. The low pressure refrigerant then returns to the compressor through the low temperature counter-flow heat exchanger where it is warmed back up to room temperature. The refrigeration capacity will be controlled by variable speed compressors. Temperature uniformity across the focal plane is adjusted using individual electrical trim heaters. For long term reliability, the cold regions of the system are protected from plugging with frozen lubricating oil by the use of a patented oil separator [15] based on fractional distillation. Using available commercial hermetic compressors limits the cycle to 120 watts at 140K. A cluster of 6 or 8 identical independent refrigeration units are used to carry the full 700 watt cryogenic heat load. A similar dual unit removes 400 watts from the raft control crates at -35 to -40°C using standard R507 refrigerant.

5.2 Contamination Control

The need to place all front end and digitizing electronics within the cryostat demands unprecedented control of the vacuum environment in order to guarantee image consistency between calibrations. The fundamental design issue is to slow the rate at which condensable molecules such as H₂O will deposit on the cold focal plane, and to reduce altogether those contaminants which are non-evaporable. Four engineering mitigations have been adopted: i) thermal design/control to maintain the focal plane at a higher temperature than the surroundings, ii) creation of two distinct vacuum regions in the cryostat (“clean-focal plane region” and “insulating region”), and reducing the conductance paths between them, iii) strict selection of all materials and control of their preparation and integration to minimize the sources of contaminants, and iv) the use of ‘getter’ sorption pumps.

To quantify and limit the total outgassing, especially condensables, these properties must be measured for all candidate materials. A camera materials test chamber [16], has been developed to perform measurements of the outgassing and deposition properties of material samples. Testing will be executed to quantify the projected gas load of all molecular species (scaling to the actual dimensions in the cryostat), and to disqualify materials which would lead to unacceptably high gas loads, significant condensables on the focal plane, or that desorb non-evaporable molecules.

A comprehensive quality assurance and performance plan will be executed to ensure that cleanliness requirements are met. This includes handling, cleaning, bake-out, and storage procedures, as well as retesting of completed sub-assemblies. The sample testing program described above, provides the acceptable baselines for the handling and processing procedures of small subcomponents, while a distinct sub-assembly test chamber will be developed for production testing. Systematically developed and documented testing, handling, and bake-out procedures will ensure that final gas loads are consistent with those measured from sample materials, and are in line with the engineering specifications for the system.

To further reduce the gas load near the focal plane, a getter pump is built into the cryostat. A re-generable molecular sieve system is in place in the focal plane region itself, while a cold activated charcoal evaporable system resides in the pumping plenum region. A program of testing to quantify the absorption properties of these getter materials is established, and the sorption pump structures will be designed to mitigate the estimated outgassing loads derived from the materials testing program data. Prototypes of the sorption pump structures will verify the crucial issues of pumping performance, containment of dust, and, in the case of the zeolite structure, effective isolation and regeneration.

6. OPTICS

The camera optics design includes four optical elements. First, the large L1 and L2 refractive lenses are mounted at the entrance to the camera, and minimize chromatic effects of L3 and the filters. These are followed by interchangeable broad-band filters. Five filters are stored on-board the camera, allowing for quick filter changes during observing runs to provide spectral coverage from the ultraviolet to near-infrared. Finally the L3 lens serves as a window and vacuum barrier for the cryostat containing the cooled detector array.

6.1 L1/L2 Assembly

The large L1 and L2 lenses are housed in a separate sub-assembly at the front end of the camera. The L1 lens has a clear aperture radius of 775 mm and forms the window into the camera volume. The diameter is nearly that of the camera itself. With a clear aperture radius of 551 mm, L2 is significantly smaller in diameter, but is still large and heavy. The two lenses are supported off a toroidal ring with a triangular cross-section. Each lens is mounted to the ring by way of

flexures which isolate the lenses from forces and moments due to distortions of the ring and changes in temperature, while providing azimuthal and axial positioning. The entire sub-assembly is kinematically supported off the front end of the camera housing by a hexapod of adjustable struts. The struts provide a stiff support to minimize gravity-induced deflection, while also reducing motions due to changes in temperature. They include flexures at either end to reduce bending forces, and differential-screw adjusters to provide fine-adjustment capability without sacrificing strength or stiffness.

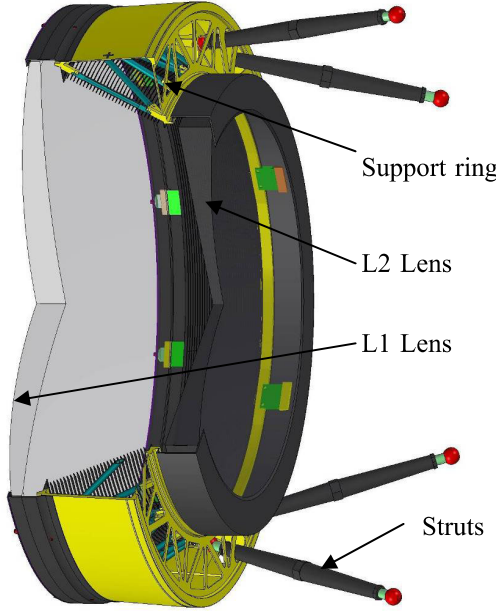


Figure 11. L1-L2 Assembly.

6.2 L3 Lens Assembly

L3 is the smallest lens, with a clear aperture of 690 mm. It also is the vacuum barrier for the cryostat containing the detector array, which is spaced 28.5 mm off the inner surface of L3. As with the filters, the L3 lens is supported in a frame that, in this case, also forms the front flange of the cryostat. The vacuum side of the lens rests on a viton gasket around its perimeter which forms a vacuum seal and also carries the vacuum load of the lens. The gasket is thick enough that it shears to accommodate the differential expansion between the flange and lens. On the air side of the lens, a clamp ring with O-ring captures the perimeter of the lens.

6.3 Filters

The ugrizy LSST filter complement, described in a companion paper in these proceedings [5], and summarized in Table 1 and Figure 12, is modeled after the Sloan Digital Sky Survey (SDSS) system [17] with an extension to longer wavelengths.

The filters utilize multi-layer interference coatings to transmit only light with wavelengths in a specified band, and to reject light at other wavelengths with a specified fidelity. These are deposited on the front and back surfaces of a curved substrate fabricated from fused silica with a clear aperture of 756 mm. The main challenge for the fabrication of the filters is to deposit uniform coatings with the desired characteristics on such large substrates. We are currently engaged in development plans with two prospective filter vendors to engineer the required fabrication strategy.

Table 1. Baseline LSST filter band-pass FWHM points in nm.

Filter	λ_1	λ_2
u	330	400
g	402	552
r	552	691
i	691	818
z	818	922
y	970	1060

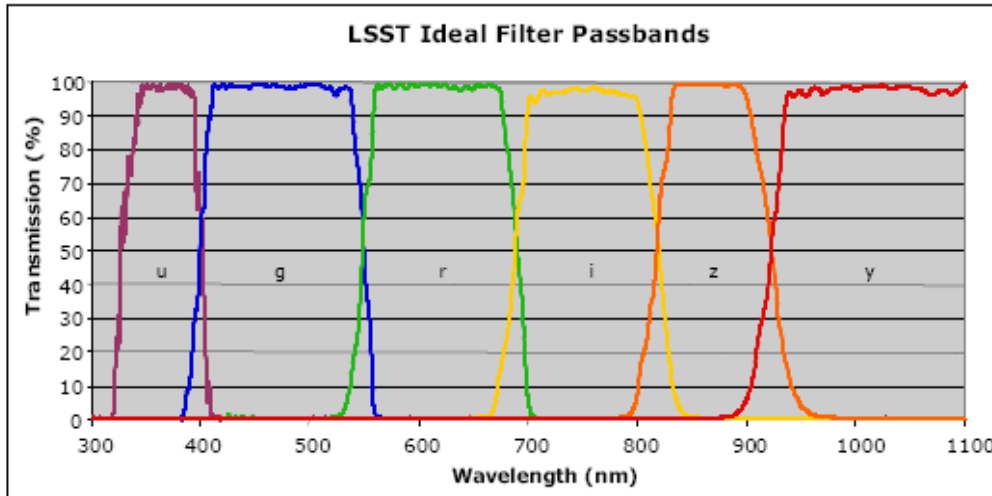


Figure 12. The LSST Filter Passbands.

7. FILTER EXCHANGE SYSTEM

The LSST camera houses five on-board filters for fast filter changing during nightly viewing, and includes the capability for swapping in a sixth filter during daytime maintenance access. The filter exchange system includes three sub-assemblies to provide this functionality. The carousel holds the filters that are not in use and moves them into position for placing on-line when needed (Figure 13). The filters sit in cradles on a ring bearing that surrounds the cryostat, with the filters oriented 90° to their on-line position. The selected filter is moved into the light beam by the auto changer (Figure 13). This mechanism grabs the filter while it sits in its slot in the carousel, then moves it forward and pivots it into its final position between the L2 and L3 lenses. Finally, a manual changer is used for swapping out a filter during daytime access. The manual changer engages with the internal auto changer rails to ensure a smooth and safe hand-off of the filter. All three of these assemblies ensure that the large-diameter filters are handled safely, and can be accessed and brought on-line quickly to maximize viewing time.

The mechanical design of the filter exchange assemblies has been largely driven by three requirements. First, the primary derived requirement for the system is that any of five filters can be inserted into the on-line position in less than 120 seconds. This relatively fast change-out time is one of a number of important parameters to maximize the cadence of image-taking during nightly viewing, which is essential for a survey telescope such as LSST. There will be 10-15 filter changes per night, so just the act of changing filters will use about 5% of the nightly viewing time.

Second, the large size of the focal plane and filter clear aperture significantly impacts all aspects of the design of the filter exchange system. The large size relative to the diameter of the camera body places constraints both on the external volume for moving the filter around, and the space around the filter for support and manipulation, because of the large clear aperture and field of view.

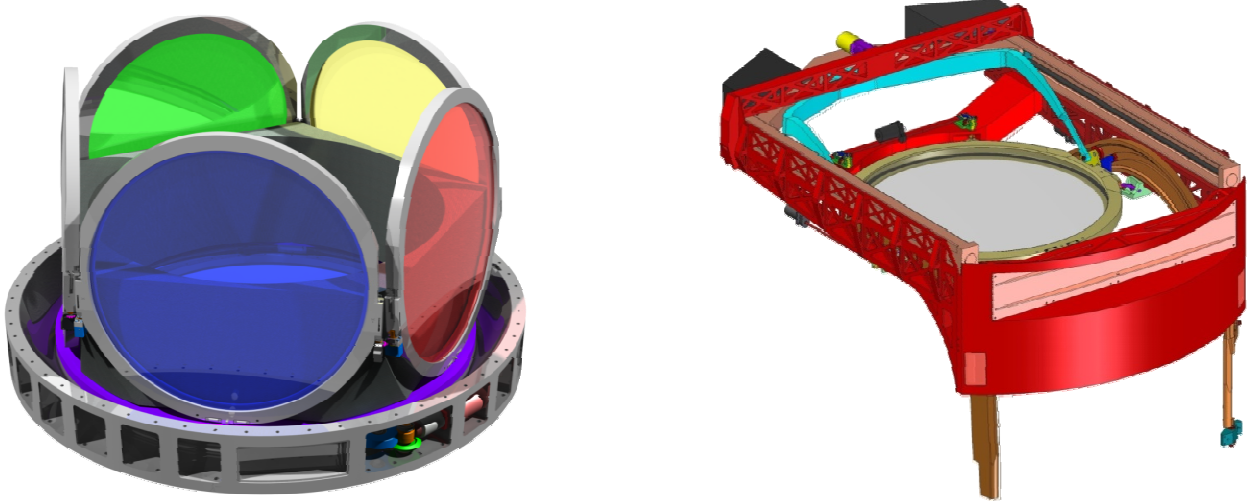


Figure 13. Filter carousel and auto-changer.

Finally, along with handling the large filters, the exchange system must fit within the envelope of the camera and clear the bore of the telescope's secondary mirror. To meet the tight constraints on physical packaging of the filters, the exchange system shuttles filters from their storage carousel, forward and around the edge of the cryostat and L3 lens, to the on-line position between the L2 and L3 lenses. This system includes handing off the filter from the carousel storage mechanism to the auto changer. While simple one degree-of-freedom linear rail systems may work for cameras with smaller focal planes, such planar systems use far too large a footprint to fit into the constrained volume of the LSST camera. This has been the primary driver in designing a more complex three degree-of-freedom system. This system includes the carousel which holds up to five filters and rotates around the camera's bore axis to place the selected filter in the hand-off position. The filters are arrayed around the bore axis in a pentagonal configuration, facing radially inward towards the center of the camera. The carousel includes fail-safe clamps to hold the filters in place while they are in this off-line position.

The auto changer mechanism provides the second and third actuated degrees of freedom to move a selected filter from its parked position in the carousel forward and around L3 into the on-line position. To do this, the changer must translate the filter along a curved path as well as rotate it 90 degrees. Nine types of mechanisms were investigated which could produce this composite motion, including four-bar linkages, gantries, articulating "robot" arms, and various rail systems.

Ultimately, a so-called "double-rail" system was chosen. A filter is carried by a truck that rides along a set of rails which moves it into position. A second, nested rail guides an auxiliary wheel that pivots the filter. Changing the offset between the two rails alters the pivot angle of the filter. Thus, by using only one actuator to drive the trucks along their rails, the filter is moved into position while undergoing a coordinated rotation, clearing neighboring obstacles. The path of the rails in the double-rail mechanism can be designed to produce nearly any filter path necessary. In particular, the path of the filter must clear the edge of the shutter frame, while still not colliding with the L2 lens on the leading edge or the outer housing of the camera at the trailing edge. This design flexibility has proven invaluable in modifying the path of travel to clear obstacles as component designs change.

Overall the double-rail auto changer design, coupled with the storage carousel, has proven to be the only viable option of the many investigated. This provides a robust solution to an otherwise-intractable packaging problem, while providing the fast filter exchange time and long-lived design needed for operations in a survey camera.

8. CAMERA SHUTTER

For maximum spatial and photometric resolution, the LSST uses a mechanical shutter. The shutter has rectangular carbon fiber blades guided on linear bearings and driven by servo or stepper motors through toothed belts. Separate opening and closing blade systems sweep across the focal plane from parked positions at opposite ends of a common track to open and close the shutter. The LSST camera focal plane is 750 mm in diameter and parking space is limited, so

the shutter blades are divided into 3 sections that are stacked one above the other in their parked position. A single motor drives each group of 3 blade sections. Motions of the sections are coordinated during deployment by 3 different drive belt wheel diameters on the corresponding motor's belt capstan.

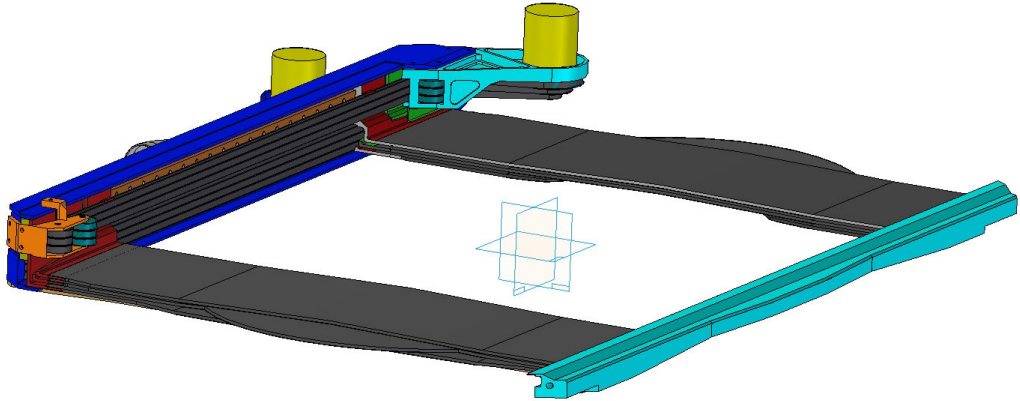


Figure14. Shutter mechanism in open position.

It is estimated that the shutter will average 400,000 exposures/year. Minimum exposure time is specified as 5 seconds with opening/closing times of 1 second. The main performance criteria are reliability and exposure uniformity over the camera focal plane. To minimize wear and vibration, a triangular acceleration drive torque profile is used which leads to a smooth blade velocity profile.

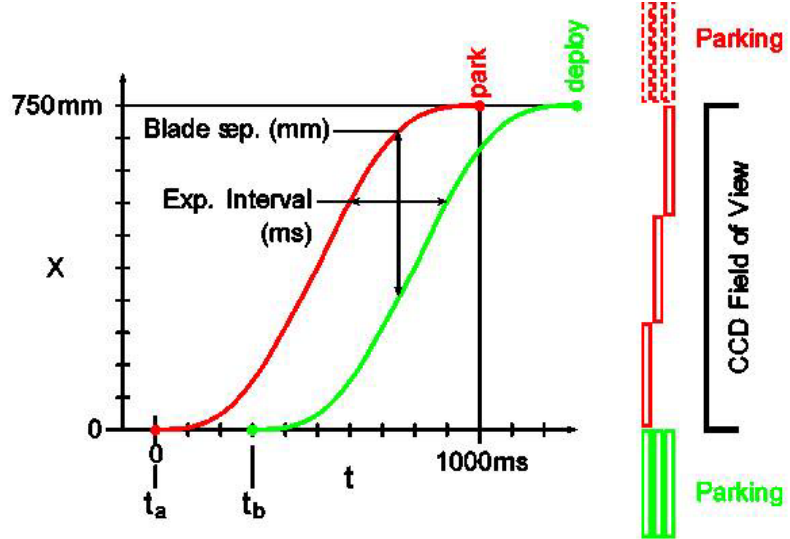


Figure 15. Shutter blade motion profile. Exposure begins with retraction of red blades from deployed position to parked position. Exposure ends with deployment of green blades from their parked position. Green blades retract to start the next exposure.

Blade velocities vary over the focal plane as they accelerate and decelerate but uniformity of exposure depends only on the interval between motion of the opening and closing blade edges. So long as opening and closing blade edge trajectories are identical, exposure is identical over the entire focal plane. Light intensity at each pixel would extinguish instantly if the shutter were mounted at the focal plane. The LSST shutter is mounted outside the cryostat vacuum forward of lens L3 about 100 mm in front of the focal plane. This causes gradual extinction of light at each pixel as the moving blade edge vignettes the light cone focused at that pixel. The time profiles of pixel light intensity vary across the focal plane. Nevertheless, all pixel intensity integrals are the same so long as opening and closing blade trajectories are the same [18].

Hall Switch proximity sensors similar to those used in modern automotive ignition systems are used to monitor blade motion. Three stationary Hall Switch sensors mounted along the blade guide track monitor the entire blade stroke by sensing the passage of a comb array of 8 to 10 small Neodymium-Fe magnets attached to the side edge of the passing blade. A train of switching pulses is emitted by each Hall Switch as individual magnets pass by. Pre-calibration of blade position at the passage of each magnet allow the trajectory to be reconstructed from the recorded Hall switching times. This technique is free of mechanical contacts or light interference. Hall switching times are sub-microsecond. Magnetic switching fields are typically 30 to 40 gauss. With the proper field configuration, switching positions should be stable to better than 0.1 mm independent of temperature or Earth's magnetic field.

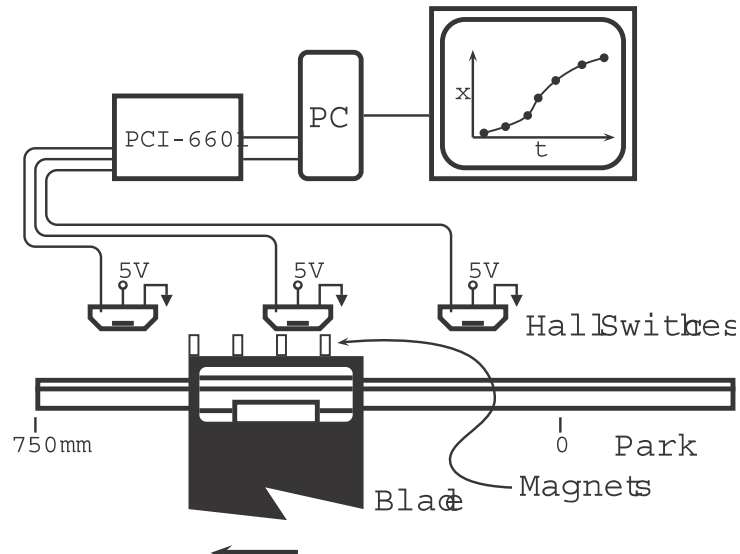


Figure 16. Hall Switch shutter blade motion monitor

9. CAMERA CONTROL SYSTEM

The LSST Camera Control System (CCS) controls and coordinates the various camera subsystems. It ensures that data acquisition operations, during both the science and calibration operating modes, proceed efficiently. The CCS monitors camera performance, maintaining a stable camera environment and reporting errors. It also interacts with the LSST telescope and data management subsystems, sending and receiving the data necessary for coordinated operations. It provides human interfaces both for the display of status information and to provide test, diagnostic, and debug capability.

The CCS architecture consists of three main types of communications:

- Data flow. Image data is high rate. Telemetry and messaging is not.
- Command. Response latency is the important parameter.
- Timing. Time stability is important.

The core CCS infrastructure component provides a set of "buses" used to transport messages between components. These buses are implemented on a TCP/IP network by a distributed set of Java processes. The types of messages include commands, status, logging and alarms. The infrastructure includes mechanisms to control write access (commands), dependencies between components, and (re)configuration.

The CCS controls camera subsystems by representing them as a set of "devices". Each CCS device is implemented as a Java process using the bus infrastructure to receive commands and communicate status information. A CCS device includes software modules specific to the subsystem hardware. For example, a subsystem containing a limit switch must have a software module that can determine the state of that limit switch. Each CCS device is a slave to a master CCS process. A CCS device is responsible for managing the hardware and responding to commands.

The third class of CCS component is a "console". A CCS console is a Java process that is capable of gathering and aggregating status messages and issuing commands to devices. In the simplest form, a command line program could allow an engineer to see the status of a CCS device and issue commands to that device. During normal observing, the "OCS Console" will run and provide the interface that allows the Camera to operate as a service to the Observatory Control System.

10. DATA ACQUISITION SYSTEM

The principal function of the Data Acquisition (DAQ) System is to both acquire and process incoming CCD science data from the camera and deliver those data, using commodity network interfaces and protocol to LSST's Data Management (DM) System [2]. The camera reads out its entire focal-plane array in no more than two seconds. This amounts to a total throughput requirement of 6.432 Gbytes/sec for the entire DAQ system. Although not strictly required, the DAQ system is capable of sustaining this rate continuously. The system is itself physically distributed with functionality spread over three independent locations. This functionality includes:

- The Raft Communication Interface (RCI) operating within the camera.
- The Science Data System (SDS) operating at the mountain-top, but off the camera.
- The Data Management Interface (DMI) operating at the LSST base-camp.

Processing of camera CCD data takes place in the SDS and includes reformatting to reflect the physical topology of the CCD focal-plane array as well as performing a real-time, cross-talk correction. In order for observatory operations to continue uninterrupted when faced with an outage between mountain-top and base-camp, the SDS is itself capable of buffering as many as three days worth of camera images.

The bulk of the DAQ System resides in the SDS. However, some components reside as firmware in the camera (the RDI) and software in the DM System (the DMI). Physically the SDS consists of approximately 30 ATCA boards, two of which are used to actually receive and process incoming CCD data with the remainder providing 60-Tbytes of high performance archival storage. The processed CCD data is made available to the DM System through multiple channels of 10-G Ethernet. The processing, management and storage of those data is carried out by a network of more than 450 nodes of RCE. The entire SDS is housed in as few as three, fourteen-slot ATCA shelves (or crates), which in turn are housed in a single 19 inch rack. The DAQ System must be able to sustain a total throughput of more than 6 Gbytes/sec.

11. PLANNING FOR INTEGRATION AND TEST

The camera is comprised of two primary subassemblies: The camera body and the cryostat. The cryostat contains the detector plane sensors, analog and digital electronics, as well as structural support and thermal control hardware. The 25 sensor raft towers are fully independent modules that can be integrated and individually tested in any order across the focal plane. The camera body provides structural support for the entire camera, serving as the primary mount point for the L1-L2 lens assembly, shutter, and filter exchange system. These are integrated into the camera body before the cryostat is inserted, allowing for parallel assembly and testing of these mechanisms. Finally, the completed cryostat is inserted into the loaded camera body in a single operation, completing the camera.

Three key design principles have guided the camera design as it has evolved and been refined. First, the camera components should be modular and self-contained. This allows for independent assembly of the components and assemblies at remote locations within the collaboration, as well as early in-process testing of the modules before being integrated into the camera. That reduces the risk of problems occurring during camera integration, and also speeds the final integration process. Component modularity additionally improves serviceability by reducing the mechanical interdependencies between components, and allows them to be serviced and removed with minimal disturbance of neighboring components.

Second, only pre-tested and verified sub-assemblies and components are integrated into the camera assembly. All key camera sub-assemblies are both functionally and performance tested prior to installing in the camera, thereby minimizing the risk of early failures and the need for disassembly during follow-on integration work and early commissioning. Furthermore, performance is again verified after integration in the camera, but before subsequent work is performed. Such incremental testing ensures that the outcome of each integration step is verified to be successful, and that any process or procedural problems are detected and corrected early.

Third, early planning for integration and testing—and the related servicing activities during operations—is essential during the development phase, and provides a strong base for implementing the design and starting construction. The camera mechanical package is heavily constrained by its optical and structural requirements, and the control systems require tight inter-relationships among subsystems. Thus, planning for and understanding how these are brought together and tested is required to ensure that they operate as expected when they have been fully assembled.

12. CONCLUDING COMMENTS

The LSST camera is a very large, complex instrument, whose design has been driven by a number of significant implementation challenges. When its fabrication is completed, it will be the largest digital visible-band astronomical camera in the world, and is likely to hold that position for a number of years. We are presently engaged in a detailed research and development program designed to identify and mitigate the numerous technical risks that the camera design presents. According to our present schedule, the camera will be delivered to the mountain in 2016 for implementation on the telescope in early 2017.

ACKNOWLEDGEMENT

LSST is a public-private partnership. Funding for design and development activity comes from the National Science Foundation, private donations, grants to universities, and in-kind support at Department of Energy laboratories and other LSSTC Institutional Members. This work is supported by the U.S. Department of Energy under contract DE-AC02-76SF00515 with the SLAC National Accelerator Laboratory, contract DE-AC02-98CH10886 with Brookhaven National Laboratory, with the Lawrence Livermore National Laboratory under the auspices of the U.S. Department of Energy under Contract DEAC52-07NA27344 and in part by the U.S. Department of Energy Office of High Energy Physics under grant DE-FG02-91ER40681A29 awarded to Purdue University. Portion of this work was also supported in part by Purdue University.

REFERENCES

- [1] Z. Ivezi, J.A. Tyson, et al., “LSST: From Science Drivers to Reference Design and Anticipated Data Products”, *Astro-ph/0805.2366*, 2008.
- [2] Kantor, J., Axelrod, T., “An overview of the LSST data management system”, *Proc. SPIE 7740-60* (2010).
- [3] Neill, D., Krabbendam, V. “LSST telescope mount and pier design overview”, *Proc. SPIE 7733-11* (2010).
- [4] Neill, D., Hileman, E. “LSST Telescope primary/tertiary mirror cell assembly”, *Proc. SPIE 7733-95* (2010).
- [5] Gilmore, K., “Large Synoptic Survey Telescope filter design and fabrication”, *Proc. SPIE 7739-187* (2010).
- [6] Bauman, B., et al., “Update and image quality error budget for the LSST camera optical”, *Proc. SPIE 7733-102* (2010).
- [7] Riot, V., et al., “The LSST camera corner raft conceptual design: a front-end for guiding and wavefront correction”, *Proc. SPIE 7736-229* (2010).
- [8] Takacs, P., et al., “PSF and MTF measurement methods for thick CCD sensor characterization”, *Proc. SPIE 7742-07* (2010).
- [9] Kotov, I., et al., “Study of pixel area variations in prototype LSST CCDs”, *Proc. SPIE 7742-06* (2010).
- [10] Sweeney, D., et al., “Management evolution of the LSST project”, *Proc. SPIE 7738-26* (2010).
- [11] O’Connor, P., Radeka, V., Geary, J.G., Gilmore, D.K., Oliver, J., Takacs, P., and Tyson, J.A., “Study of Silicon Thickness Optimization for LSST”, *Proc. SPIE 6276, 62761W* (2006).
- [12] O’Connor, P., Frank, J., Geary, J.G., Gilmore, D.K., Kotov, I., Radeka, V., Takacs, P., and Tyson, J.A., “Characterization of prototype LSST CCDs”, *Proc. SPIE 7021, 702106* (2008).
- [13] Bowden, G. “L3 Temperature & Focal Plane IR Heat-load”, LSST Camera Engineering Note No. CE2-06 Rev 1, (2009)
- [14] MMR Technologies, 1400 North Shoreline Blvd, unit 5, Mountain View, CA 94043, www.mmr.com/kleemenko.html
- [15] United States Patent 5,617,739 “Self Cleaning Low-Temperature Refrigeration System”, William Little, 1997.
- [16] Singal et al., *Rev Sci Instrum.*, 81, 025101, 2009.
- [17] Fukugita et al., *Ast. J.*, 411/4, April 1996, p. 1748-1756.
- [18] G. Bowden, “Shutter Blade Trajectory”, LSST Camera Engineering Note No. CE5-09, August 2010.